Journal of Chemistry

WILEY

RESEARCH ARTICLE OPEN ACCESS

Using Pozzolanic Materials to Improve Mechanical Properties of Lime-Based Mortar

Odiwuor Vincent Onyango[1] | Ayabei Kiplagat[1] | Maurice O. Okoth[1] | Onesmus Mulwa Munyao[2]

[1]Department of Chemistry and Biochemistry, University of Eldoret, P.O. Box 1125-301, Eldoret, Kenya | [2]Department of Chemistry, Kenyatta University, P.O. Box 43844-00100, Nairobi, Kenya

Correspondence: Odiwuor Vincent Onyango (vincentodiwuor623@gmail.com)

Received: 22 January 2026 | **Revised:** 15 April 2026 | **Accepted:** 12 June 2026

Academic Editor: Munmun Bardhan

Keywords: durability | lime-based binders | mechanical properties | pozzolanicity | rice husk ash | sugarcane bagasse ash

ABSTRACT

The environmental impact associated with the production of Portland cement has intensified interest in sustainable alternatives such as lime-based binders. However, their application is constrained by low early strength and slow hardening. This study evaluates rice husk ash (RHA) and sugarcane bagasse ash (SCBA) as pozzolanic additives to enhance the mechanical performance and durability of lime mortars. Hydrated lime was partially replaced (50%) with RHA or SCBA, and the mortars were air-cured for 28 days. Both ashes satisfied the standard pozzolanicity requirements. RHA exhibited a higher amorphous silica content and greater reactivity, whereas SCBA demonstrated slower but sustained pozzolanic activity. The incorporation of these pozzolans significantly improved performance. Compressive strength increased from 0.43 MPa for pure lime to 4.64 and 3.84 MPa for RHA and SCBA mortars, respectively. Flexural strength improved from 0.17 to 2.70 MPa and 0.97 MPa for RHA and SCBA mortars, respectively. Water absorption was substantially reduced in the modified mortars, indicating improved pore structure and durability. RHA provided superior strength development and lower permeability, while SCBA offered moderate strength enhancement with improved flexibility. These characteristics make both materials suitable for nonstructural applications, including heritage conservation and restoration. The findings demonstrate that agricultural waste ashes can serve as effective, low-carbon pozzolanic materials for durable lime-based construction.

1 | Introduction

Concrete and mortar remain among the most widely used construction materials due to their strength and adaptability to diverse environmental conditions [1]. Hydrated lime and cement are fundamental components in mortar production. Cement-based mortars are particularly favored because of their rapid setting and high compressive strength [2]. However, cement production is highly energy-intensive and a major contributor to global CO_2 emissions, arising from both limestone calcination and fossil fuel combustion. As a result, the cement industry is recognized as one of the largest sources of anthropogenic CO_2 emissions [3].

These environmental concerns have driven increasing interest in low-carbon alternative binders. Lime-based systems have re-emerged as promising candidates due to their lower embodied CO_2, which results from reduced calcination temperatures and energy demand compared to Portland cement [4–6]. However, lime mortars are not intended as universal replacements for cement. Instead, they are better suited to specific applications such as heritage conservation, masonry repair, and breathable construction systems. Their advantages include compatibility with historic substrates, vapor permeability, and good workability [5, 6]. Despite these benefits, the broader application of lime mortars is limited by low early strength, slow hardening,

and reduced resistance to moisture. To address these limitations, research has focused on enhancing lime-based binders through the incorporation of pozzolanic materials, fibers, and organic additives [7, 8]. Pozzolans react with calcium hydroxide to form strength-enhancing hydrates, improving both mechanical performance and durability.

Several studies have examined how lime binders behave when blended with both natural and industrial pozzolanic materials. Traditional pozzolanic materials such as fly ash, silica fume, and metakaolin have been extensively studied [9–15]. Collectively, these studies have consistently shown that adding pozzolans improves the hydraulic behavior of lime-based binders. This improvement comes from their reaction with calcium hydroxide to form strength-giving hydrates, while also helping to control heat release, accelerate early strength gain, and support better long-term durability [16]. While effective, long-term availability of industrial byproducts and natural pozzolans is becoming uncertain due to regulatory constraints and competing industrial demands [15]. Consequently, attention has shifted toward agricultural waste materials such as rice husk ash (RHA) and sugarcane bagasse ash (SCBA), which are abundant, renewable, and rich in reactive amorphous silica [14, 17].

RHA is widely recognized for its high reactivity and ability to significantly enhance strength and microstructural densification in lime-based systems. In contrast, SCBA typically exhibits slower early-age reactivity but contributes to sustained strength development over time, particularly when properly processed through controlled calcination and grinding. Although both materials have been studied individually in stabilizing lime and cement systems [14, 17, 18], there are still relatively few directly comparable datasets produced using the same experimental conditions. Variations in mix design, curing conditions, and processing methods have hindered meaningful comparison of their relative performance. As a result, their relative pozzolanic efficiency and strength development performance are not yet well understood. This gap restricts the rational selection of suitable agricultural pozzolans for sustainable construction applications. This highlights the importance of carrying out a well-controlled, side-by-side comparative evaluation.

Accordingly, a systematic comparative evaluation of SCBA and RHA-modified lime binders is undertaken to clarify their relative performance in terms of mechanical strength and durability. The present study comparatively assesses the effects of SCBA and RHA as individual pozzolanic additives in lime-based mortars within their appropriate application scope. Instead of introducing a completely new binder system, this study focuses on generating carefully controlled comparative data using the same mix designs and curing conditions throughout. It evaluates compressive strength, flexural strength, and water resistance in lime mortars modified with RHA and SCBA, with special emphasis on SCBA–lime blends, which have been reported less often in existing research.

By focusing on these complementary performance indicators, the study moves beyond single-property assessments and supports more informed material design decisions. By directly comparing the performance of these two widely available agricultural ashes under identical experimental conditions, this study contributes to the current understanding of their pozzolanic efficiency and practical suitability, thereby supporting more rational selection of agricultural pozzolans in lime-based construction materials. Ultimately, this study seeks to provide experimental evidence that can guide more informed and technically grounded choices in the design of lime-based mortar materials.

2 | Methods

2.1 | Sample Preparation

Rice husks were first cleaned through sieving, air separation, and washing to eliminate larger debris, lightweight contaminants, and surface dust. They were then left to sun-dry for 2 days and subsequently dried in an oven at 110°C for 24 h. The sugarcane bagasse was milled using an HFM 100 grinder (Beijing Grinder Instrument Co., Ltd., Beijing, China), after which it was also sun-dried for 2 days and oven-dried at 110°C for 24 h. Both the prepared rice husk and bagasse were then calcined separately at 600°C for 2 h in a muffle furnace (OSK 9540-MK-SP 38351) to obtain RHA and SCBA. Following calcination, the resulting RHA and SCBA were allowed to cool gradually for 24 h to room temperature. To optimize the fineness and reactivity of the pozzolans, the resulting ashes were subjected to a mechanical grinding process using a laboratory-scale ball mill operated at a constant speed of 300 RPM for a duration of 30 min. The milling was conducted at a constant speed to ensure the production of a fine, homogeneous powder with a particle size below 75 μm, ensuring uniform dispersion in the mortar mixes.

2.2 | Physical Analysis

The particle size distribution (PSD) of the pozzolans was measured using a sieve analyzer with a series of sieve sizes (1180, 850, 600, 425, 300, 212, 150, and 75 μm). This procedure allowed for grading the materials and ensuring they met the required specifications. The specific surface area (SSA) was determined using a Brunauer–Emmett–Teller (BET) nitrogen adsorption analyzer (Gemini 2375 V.).

2.3 | Determination of Lime, RHA, and SCBA Oxides and Loss on Ignition (LOI)

The chemical composition of the pozzolanic materials and lime was determined using X-ray fluorescence (XRF) analysis. Measurements were carried out with an MXF-2400 spectrometer (Shimadzu, Kyoto, Japan). For sample preparation, 0.9 g of each pozzolan was accurately weighed into a platinum crucible and mixed with 9.0 g of lithium tetraborate flux. The mixture was fused in an M4 gas fusion unit for 17 min to obtain a homogeneous glass bead. After fusion, the beads were cooled in a desiccator and subsequently analyzed using the XRF instrument. Each cementitious material was tested in triplicate, and the average values were calculated and reported in Table 1. LOI was determined for each test sample using three replicate specimens, following the gravimetric procedure specified in KS EAS 18:1-:2017 [19]. For each measurement, 1.0 g of each test sample was accurately weighed and placed in a preweighed, tared silica crucible. The crucible and sample were heated in a furnace at 975°C for 1 h and then allowed to cool in a desiccator. The LOI was calculated as the percentage mass loss between the initial and final weights.

2.4 | Mineralogical Analysis

The mineralogical composition of the lime and pozzolanic materials was characterized using X-ray diffraction (XRD). Prior to testing, the samples were oven-dried at 100°C and ground to a fine powder using an electric grinder and then mounted in a zero-background silicon sample holder. The goniometer was calibrated using a silicon reference standard. XRD data were collected and analyzed with an XRD (SmartLab SE, Rigaku, Tokyo, Japan). Scanning was performed over a 2θ range of 5.00°–80.002°, using a step size of 0.0202° and a step time of 0.5 s, under operating conditions of 40 mA and 35 kV.

2.5 | Reactivity by Electrical Conductivity

A rapid assessment of pozzolanic reactivity was conducted by monitoring changes in the electrical conductivity of a saturated calcium hydroxide solution, following the procedure proposed by Luxán et al. [20]. In this test, 200 mL of distilled water was placed in a 500-mL glass beaker and heated on a magnetic hot plate to 40 ± 1°C. Calcium hydroxide was then gradually added until saturation was achieved. The solution was magnetically stirred for 2 min, after which its initial electrical conductivity was measured using a conductivity meter (SIBATA Model SC-17 A). Subsequently, 5.0 g of the pozzolanic material was added to the saturated calcium hydroxide solution, which was maintained at 40 ± 1°C, and the suspension was continuously stirred for an additional 2 min. Electrical conductivity readings were recorded at 30-min intervals over a period of 4 h. Pozzolanic activity was evaluated based on the difference between the conductivity of the saturated calcium hydroxide solution and that of the suspension containing the pozzolanic material. All measurements were performed in triplicate, and the results are presented as mean values along with their corresponding standard deviations.

2.6 | Mix Proportions

The mortar mixtures were prepared using hydrated lime as the main binder, with agricultural waste ashes serving as supplementary pozzolanic additives. SCBA and RHA were incorporated as partial replacements for lime in the blended systems, while a control mixture containing only hydrated lime was also prepared for comparison. All mortars were designed with a binder-to-fine aggregate ratio of 1:3 by mass. In the blended mortars, 50% of the lime was substituted by the pozzolanic material, resulting in binders composed of equal parts hydrated lime and the respective ash (1:1 by mass). This 1:1 replacement ratio was chosen to provide enough reactive silica and alumina from the pozzolans while maintaining sufficient calcium hydroxide to support the pozzolanic reaction. A uniform water-to-binder ratio of 0.50 was used across all mixtures to ensure consistent workability and allow for direct comparison of performance. The specific mix proportions are summarized in Table 2.

In the blended mortars, the binder portion includes both the lime and the pozzolanic material, with lime replaced by 50% of the pozzolan by mass. All mix proportions are given relative to the total binder mass.

2.7 | Mortar Preparation

Mortar prisms were prepared and cast following the Kenyan standard KS EAS 2168-1:2020 [21], with minor modifications applied. To ensure a homogeneous binder, hydrated lime was first blended with the pozzolanic additives in the proportions listed in Table 2. The binder was composed of 1350 g of graded sand and 450 g of a pozzolan–hydrated lime mixture in a 1:1 mass ratio. Mixing was carried out in an automatic mortar mixer for 90 s. The fresh mortar was then placed into greased three-part molds with dimensions of 40 × 40 × 160 mm, and each layer was compacted using 20 strokes of a steel tamping rod. For the first two days after casting, the specimens were kept in their molds under high-humidity conditions of about 95 ± 5%. After 48 h, the specimens were removed from the molds and cured at a relative humidity (RH) of 60 ± 5% and a temperature of 20 ± 2°C, following the procedures outlined in ASTM C109 [22]. Specimens were cured in air at around 60% RH to mimic real-world conditions for lime-based mortars, where carbonation significantly contributes to strength development. This curing approach was chosen to reflect practical field conditions rather than accelerated laboratory hydration. All lime mortar specimens were cured under air conditions for 28 days to promote carbonation. Lime-based mortars require a long curing period, so it was not possible to measure strength at 3 and 7 days. Air curing was adopted because lime-based mortars primarily gain strength through carbonation, a process that depends on exposure to atmospheric CO_2 and sufficient moisture [23]. This curing approach allows the mortars to harden in a manner that closely replicates their natural setting behavior since some researchers have suggested that using noncarbonated lime in mortar mixtures can potentially reduce the mortar's strength [24].

2.8 | Water Absorption

The water absorption of mortar specimens (40 × 40 × 160 mm) was determined following BS 1881-122 [25]. Prior to testing, the specimens were oven-dried at 60 ± 5°C until a constant mass was achieved and then cooled in a desiccator. The dry mass of each specimen was recorded as m_1. The specimens were then fully immersed in a sealed container of water for 48 h. To allow trapped air to escape, the samples were initially placed at an approximate 45° angle and subsequently positioned vertically to start the test period. After 48 h, the specimens were removed, surface water was gently wiped away with a damp cloth, and the saturated mass was recorded as m_2. Water absorption was expressed as a percentage, calculated using the standard formula shown in the following equation:

$$W_{48} = \frac{W2 - W1}{W1} \times 100. \quad (1)$$

2.9 | Determination of Flexural and Compressive Strength

The compressive strength of the cured mortar prisms was measured at 28 days following KS EAS 148-1:2000 [26]. For each curing condition, three prisms were removed from the curing environment, and any surface residues were gently wiped off with a dry woven cloth. After labeling, the specimens were placed in a compression testing machine. A preliminary vertical load of 50 N/s was applied, followed by continuous loading at a rate of 2400 N/s until failure. The compressive strength was calculated as the average of the three specimens and reported in MPa. All tests were performed using a YAW-300 compression testing machine. Flexural strength tests were conducted according to the

TABLE 1 | Physical properties (specific surface area and mean particle size) of the pozzolanic ashes.

Sample	Specific surface area (m^2/g)	Mean particle size (μm)
SCBA	33.2	252
RHA	72.1	225

standards of the EN196-1 [27], using an MTS 809 hydraulic press (MTS Systems Corporation, Eden Prairie, MN, USA). Mortar prisms measuring $40 \times 40 \times 160$ mm were used, with three samples tested per mix. The mean of the three results was reported as the final flexural strength.

2.10 | Data Analyses

All tests were performed in triplicate, and the reported mean and standard deviation values were calculated from the three measurements. Statistical comparisons between the mean values of the cement pastes containing the selected pozzolans were carried out using an independent two-sample, two-tailed t-test at a 95% confidence level. Differences were considered statistically significant when $p < 0.05$. The statistical analyses were conducted in SPSS, and the outcomes were presented using appropriate statistical tables, as well as line and bar charts.

3 | Results and Discussion

3.1 | Physical Characterization of the Materials

Evaluating PSD and SSA helps to understand the fineness, grading, and potential reactivity of pozzolanic materials, which are key factors in their effectiveness as supplementary cementitious materials. Table 1 presents the average particle size and SSA values for SCBA and RHA.

Particle fineness plays a major role in pozzolanic reaction rates because a higher SSA provides a more reactive surface and allows amorphous silica phases to dissolve more quickly [28]. In this study, the RHA showed a higher SSA than SCBA (72.1 vs. 33.2 m^2/g) and also had a slightly finer average particle size. With more exposed surface available for reaction, RHA is therefore expected to be more pozzolanically active, promoting faster consumption of calcium hydroxide and contributing more effectively to strength development. By comparison, the relatively coarser SCBA particles are likely to react at a slower rate, with part of their contribution coming from a filler-type effect rather than chemical reaction [29].

The measured SSA of RHA in this study is higher than the value reported by Marangu et al. [30], who obtained 51.4 m^2/g, but far below the much larger value published by Cordeiro et al. [29], 42,738 m^2/kg. RHA typically has an angular, layered, and highly microporous texture, which explains its generally high surface area [31]. Its fine particle size and porous structure increase contact with other components in the mix, supporting stronger chemical interaction. Because of this higher reactivity, RHA can take part more readily in reaction processes and help improve the performance of cement-based materials [28].

The SSA of the SCBA used in this work (33.29 m^2/g) falls within the range reported by other researchers. For example, Yaseen [32] reported 30.55 m^2/g, while Figueiredo and Pavia[33] measured 25.64 m^2/g for SCBA. Differences in SCBA surface area are often linked to its variable particle shapes, which can include angular, prismatic, spherical, and fibrous forms [32]. The surface area values of the ashes (Table 1) follow the expected trend with PSD: Finer particles tend to produce higher SSAs. Similar patterns have been documented by Habeeb and Mahmud [31]. In another study, Habeeb and Fayyadh [34] evaluated three RHA samples with mean particle sizes of 31.3, 18.3, and 11.5 μm and measured BET surface areas of 27.4, 29.1, and 30.4 m^2/g, respectively. Rasoul et al. [35] also observed increasing BET surface area with decreasing particle size across four RHA samples. They emphasized that both SSA and particle size are key factors influencing pozzolanic reactivity in cementitious systems.

3.2 | Lime and Pozzolana Oxides

The results of the chemical analysis for the hydrated lime, test pozzolans, and the LOI expressed as a percentage by mass are presented in Table 3. The primary focus of this analysis was on the chemical composition and the LOI of the materials.

The combined $SiO_2 + Al_2O_3 + Fe_2O_3$ content of RHA was measured at 95.24%, substantially exceeding the 70% minimum requirement by ASTM C618 [36]. This high value confirmed the strong pozzolanic potential of the material. Similar silica-rich compositions, typically between 88% and 97%, have been widely reported for properly combusted RHA, particularly when burning conditions are carefully controlled to avoid silica crystallization [37–39]. SCBA recorded a combined pozzolanic oxide content of 85.77%, which also comfortably met the ASTM C618 [36] requirements. The chemical composition of SCBA obtained in this study aligns well with findings reported by Assumptor et al. [39] and Rodrigues et al. [40], supporting its suitability as a supplementary cementitious material.

Unlike RHA and SCBA, hydrated lime contains only trace amounts of reactive silica and alumina and is instead characterized by a very high CaO content. A similar elemental composition of hydrated lime has been reported in previous studies [41, 42]. Lime does not exhibit pozzolanic behavior on its own. Its primary function in blended systems is to supply calcium ions, which react with the amorphous silica and alumina present in

TABLE 2 | Mix proportions of mortar constituents (mass ratios relative to total binder content).

Mix ID	Hydrated lime	SCBA	RHA	Standard sand	Deionized water
Control (L100)	1.0	—	—	3.0	0.50
L–SCBA (50/50)	0.5	0.5	—	3.0	0.50
L–RHA (50/50)	0.5	—	0.5	3.0	0.50

Note: All proportions are expressed as mass ratios. The binder-to-aggregate ratio is maintained at 1:3, and the water-to-binder (w/b) ratio is constant at 0.50 across all mixtures to ensure comparability.

TABLE 3 | Chemical composition (wt.%) of RHA, SCBA, and hydrated lime determined by XRF analysis.

Material	SiO_2	Al_2O_3	Fe_2O_3	CaO	MgO	K_2O	Na_2O	LOI	$SiO_2 + Al_2O_3 + Fe_2O_3$
RHA	94.42 ± 0.02	0.50 ± 0.01	0.27 ± 0.01	0.70 ± 0.02	—	1.20 ± 0.02	0.32 ± 0.01	5.26 ± 0.02	95.24 ± 0.03
SCBA	84.61 ± 0.04	0.42 ± 0.01	0.74 ± 0.02	2.59 ± 0.03	—	0.94 ± 0.02	1.09 ± 0.01	11.58 ± 0.02	85.77 ± 0.04
Lime	—	1.46 ± 0.01	—	96.46 ± 0.02	—	—	—	26.14 ± 0.02	—

RHA and SCBA to form C–S–H and calcium aluminate hydrate (C–A–H) phases. These hydration products play a central role in strength development and durability enhancement in lime-based mortars [43, 44].

ASTM C618 [36] specifies that Class N pozzolans must contain at least 70% combined $SiO_2 + Al_2O_3 + Fe_2O_3$, while Class F and Class C pozzolans require a minimum of 50%. The RHA and SCBA used in this study therefore fall under class N pozzolans. The chemical composition of biomass ashes is strongly affected by factors such as soil characteristics, local environmental conditions, and the quality of the calcination process [45]. Variations in these factors can significantly influence the concentration of reactive oxides and, in turn, the pozzolanic efficiency of the ashes. As shown in Table 3, the hydrated lime used in this study is predominantly calcium-based, with a combined CaO + MgO content exceeding 80%, in compliance with EN 459-1 [46] requirements. The chemical composition of the hydrated lime used in this study is consistent with values reported by Silva et al. [41] and Al-Attar and Al-Azzawi [42]. The combined CaO + MgO content of the hydrated lime in the present study was found to be lower than the values reported by Newton and Sharp [47] and Padovnik and Bokan-Bosiljkov [48]. This indicates considerable variability in the quality of commercially available lime products.

The LOI value of 5.26% recorded for RHA suggests a moderate amount of residual carbon and indicates reasonably efficient combustion. This value falls within the range commonly reported for RHA in previous studies [38, 39, 49]. By contrast, SCBA exhibited a relatively high LOI of 11.58%, reflecting a substantial presence of unburnt carbon, a characteristic frequently associated with this material. Elevated LOI levels are known to increase water demand and may negatively affect early strength development unless additional processing measures, such as finer grinding or recalcination, are applied [29, 50]. ASTM C618 [36] permits fly ash to have an LOI of up to 12%, while BS EN 197-1 [51] limits LOI to 7%. In the present study, RHA satisfied both standards, whereas SCBA complied with the ASTM requirement. The high LOI value observed for hydrated lime (26.14%) is typical and is associated with the decomposition of calcium carbonate and the release of CO_2 during calcination, as well as subsequent hydration processes. This value is comparable to that reported by Padovnik and Bokan-Bosiljkov [48] but notably lower than the LOI reported by Newton and Sharp [47].

3.3 | Mineralogical Analysis Results

The mineralogical analysis of the precursor materials used in mortar preparation is shown in Figures 1–3. The figures show various minerals present in pure hydrated lime, RHA, and SCBA.

Figure 1 shows the XRD pattern of RHA, which is characterized by a broad diffuse hump with its highest intensity occurring between 22° and 25°. This feature is typical of amorphous silica and confirms that the silica present in the RHA is largely noncrystalline in nature. Comparable diffuse amorphous halos have been widely reported for highly reactive RHA produced under carefully controlled calcination conditions, particularly at temperatures in the range of 600°C–700°C [29, 37, 52]. The lack of sharp diffraction peaks associated with crystalline silica phases such as quartz or cristobalite indicates that silica crystallization

was minimal, suggesting combustion conditions that favored the formation of reactive amorphous SiO_2 [37, 53].

These XRD findings are consistent with the chemical composition results, which revealed a combined $SiO_2 + Al_2O_3 + Fe_2O_3$ content exceeding 95%, meeting the ASTM C618 [36] requirements for natural pozzolans. The dominance of amorphous silica, together with the high silica content, enhances the reactivity of RHA with calcium hydroxide released during lime hydration. As reported by Cordeiro et al. [29], amorphous silica readily reacts with $Ca(OH)_2$ to form secondary C–S–H gels, which contribute to strength development and microstructural refinement in both lime- and cement-based systems.

In addition, the relatively low LOI value of RHA (5.26%) suggests limited residual carbon and effective combustion, conditions that are conducive to the formation of amorphous rather than crystalline silica. This combination of low crystallinity, high pozzolanic oxide content, and acceptable LOI helps explain the enhanced mechanical performance observed in lime mortars incorporating RHA. By contrast, RHA produced at higher calcination temperatures above 800°C often shows pronounced crystalline peaks due to silica recrystallization, which leads to reduced pozzolanic activity and poorer strength development [49].

The XRD pattern of SCBA presented in Figure 2 is characterized by a pronounced broad diffuse hump spanning approximately $2\theta = 15°–35°$, which indicates the dominance of an amorphous phase typical of silica-rich ashes with good pozzolanic potential [40]. This diffuse background implies that a large fraction of the silica in SCBA is present in a noncrystalline, disordered state, a condition that enhances its reactivity in lime- and cement-based binders. In addition to the amorphous halo, faint crystalline peaks are observed at about $2\theta = 24.4°$, 27.6°, 31.2°, and 71.1°. These reflections are mainly associated with quartz (SiO_2), along with minor aluminosilicate phases such as albite or orthoclase, as confirmed through phase identification. The weak intensity of these peaks reflects a low degree of crystallinity, suggesting that the combustion and subsequent processing conditions were not severe enough to cause extensive silica crystallization. Comparable XRD patterns dominated by amorphous humps and minor quartz peaks have been widely reported for SCBA materials that exhibit satisfactory pozzolanic behavior [29, 40].

The mineralogical characteristics observed in Figure 2 are closely linked to the relatively high LOI value of SCBA (11.58%). High LOI values are commonly associated with residual unburnt carbon, which arises from incomplete combustion and is often related to moderate burning temperatures that also help to preserve the amorphous nature of silica [29, 50]. Therefore, the combination of a dominant amorphous halo and elevated LOI suggests that the SCBA was produced under combustion conditions that favored the retention of reactive amorphous silica while leaving a noticeable amount of residual carbon. By contrast, SCBA produced at higher combustion temperatures typically shows lower LOI values but a greater degree of silica crystallization, evidenced by sharper and more intense quartz peaks in XRD patterns [50]. Furthermore, the absence of high-temperature crystalline phases such as cristobalite, tridymite, and mullite phases that generally form at temperatures above 800°C supports the conclusion that the SCBA was not overburnt. The XRD and LOI results indicated that the SCBA consists predominantly of amorphous silica with a measurable amount of residual carbon, a mineralogical and thermal signature that aligns well with values reported in the literature.

The XRD pattern of the pure hydrated lime sample in Figure 3 confirms portlandite ($Ca(OH)_2$) as the dominant crystalline phase, as indicated by strong and well-defined diffraction peaks. The most intense reflection at approximately 21° 2θ is widely recognized as a characteristic feature of hydrated lime systems. Additional reflections at higher angles further demonstrate the high crystallinity and phase purity of the material. Minor peaks corresponding to calcite ($CaCO_3$) suggest partial carbonation caused by exposure to atmospheric CO_2 during handling or curing. This behavior is commonly reported even in freshly prepared lime-based materials [54]. Similar XRD patterns of pure hydrated lime have previously been reported by Padovnik and Bokan-Bosiljkov [48]. This phase composition explains the typically low early strength and long-term hardening behavior of pure lime mortars reported in previous studies.

The sharp peak profiles and low background intensity indicate limited amorphous content and minimal secondary reactions. This behavior aligns with the findings of Matschei et al. [55], who reported that pure hydrated lime typically exhibits high crystallinity unless modified with pozzolanic additives, which tend to introduce broader humps associated with amorphous C–S–H or C–A–S–H phases. In contrast to lime systems modified with pozzolanic materials, where portlandite peaks are often reduced due to its consumption in pozzolanic reactions, the persistence and high intensity of $Ca(OH)_2$ reflections in this sample indicate minimal secondary reaction and confirm the nonhydraulic nature of the binder [16, 55]. This is consistent with the absence of broad amorphous halos or peaks associated with hydraulic reaction products, reinforcing the interpretation that the material remains largely unreacted and reliant on slow carbonation for long-term strength development.

3.4 | Reactivity by Electrical Conductivity

Tables 4 and 5 show the average electrical conductivity of RHA and SCBA, and Figure 4 illustrates conductivity loss over time for each sample.

Figure 4 presents the changes in electrical conductivity measured for the lime–RHA and lime–SCBA systems, which provide an indirect indication of calcium ion consumption during pozzolanic reactions [20]. Comparable trends have been documented in previous studies by Luxán et al. [20], John [38], and Assumptor et al. [39]. The reduction in electrical conductivity observed over time is mainly associated with the gradual depletion of Ca^{2+} and OH^- ions in the pore solution as they react with the reactive silica (SiO_2) and alumina (Al_2O_3) present in the ashes. These interactions lead to the formation of C–S–H and C–A–H, which are the principal reaction products responsible for strength development and improved durability in lime-based systems.

Possible sources of error in conductivity measurements include the dissolution of ash constituents in water and the presence of soluble salts, both of which could artificially increase ionic concentrations and affect conductivity readings [33]. In this study, however, such effects were negligible. Measurements carried out on ash–water suspensions showed very low

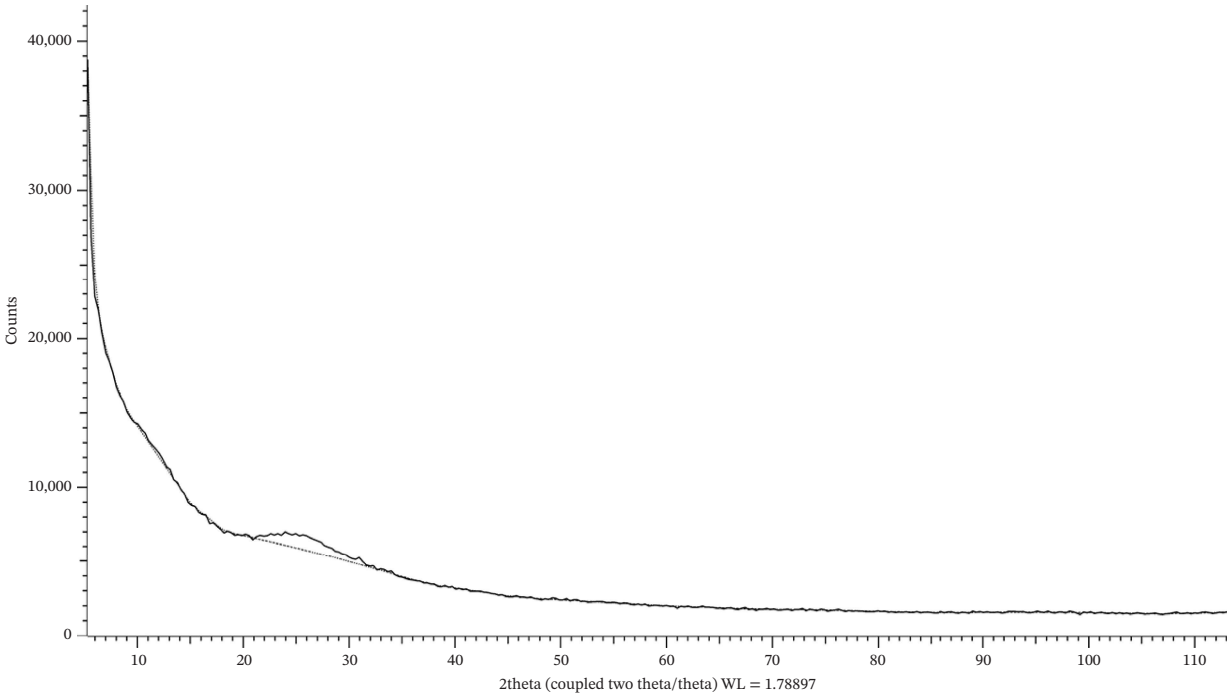

FIGURE 1 | XRD pattern of RHA.

conductivity values (< 1 mS/cm) (Tables 4 and 5), and the alkali and anion contents of the ashes were minimal, as reported in Table 3. The low conductivity readings for the ash–water suspensions by themselves confirm that the decreases observed are a result of the lime–ash reactions, rather than the inherent conductivity of the ashes. Carbonation represents another potential source of error, since atmospheric CO_2 can react with $Ca(OH)_2$ and reduce calcium availability independently of pozzolanic reactions. To limit this effect, all test suspensions were tightly sealed during the measurements to minimize CO_2

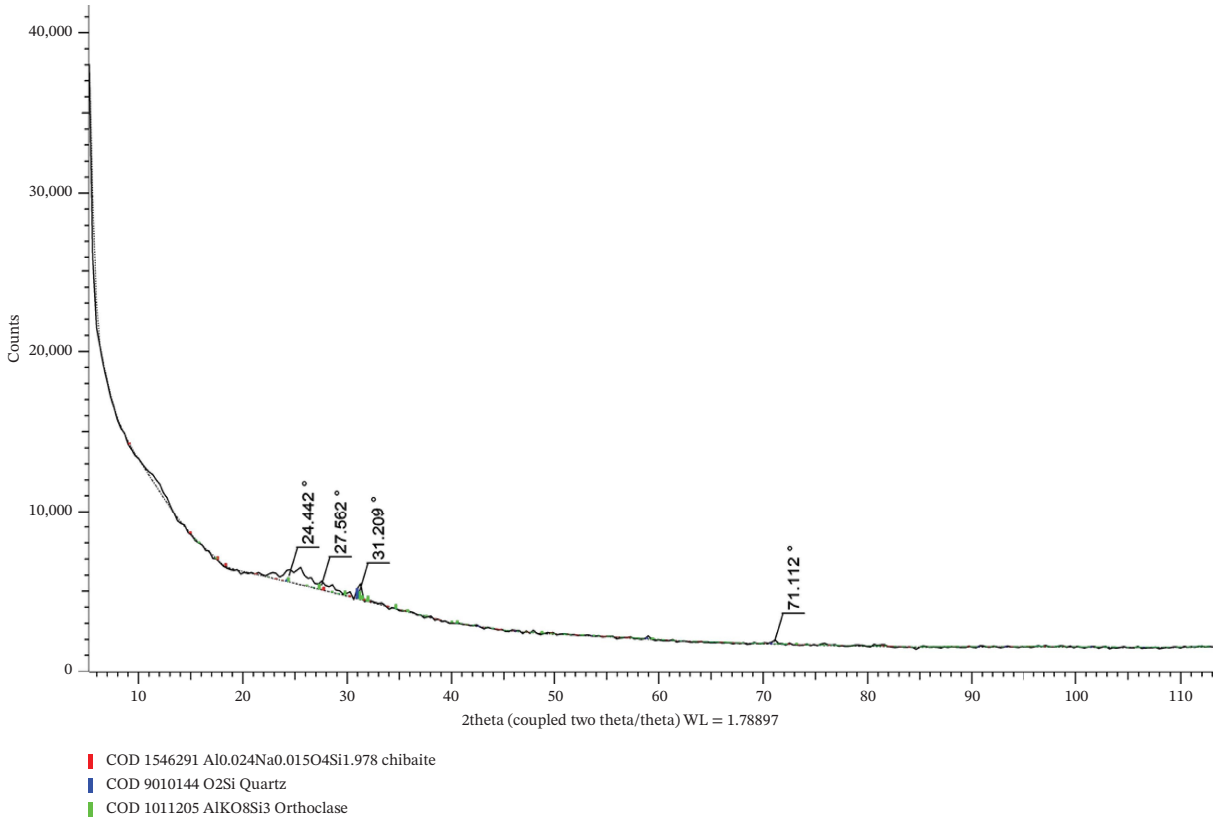

FIGURE 2 | XRD pattern of SCBA.

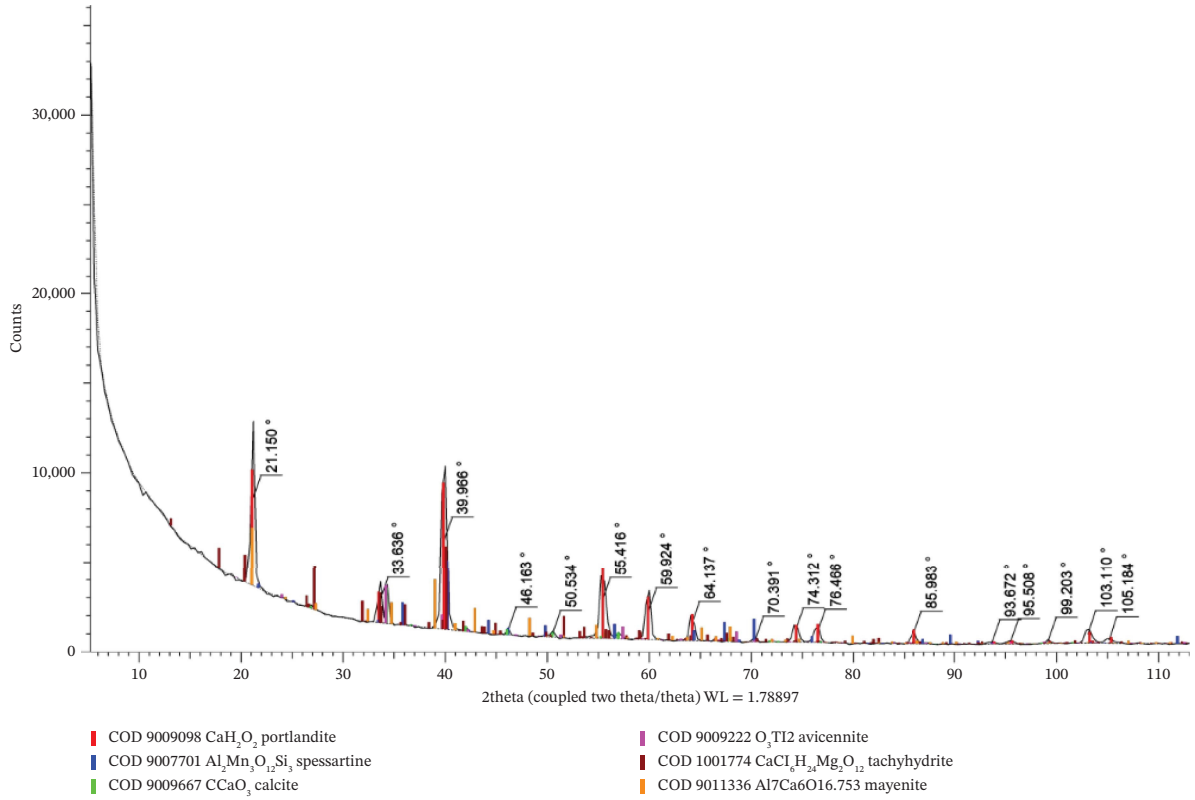

FIGURE 3 | XRD diffractogram of pure hydrated lime.

ingress. In addition, although high residual carbon contents may hinder lime–ash interactions and interfere with conductivity results, the ashes used in this study contained relatively low amounts of carbon.

Both lime–RHA and lime–SCBA systems exhibited a sharp increase in conductivity loss during the first 30 min, followed by a more gradual decline at later ages. This response indicates intense early-stage pozzolanic activity followed by sustained reaction kinetics over time. Similar behavior has been reported by Walker and Pavía [28] and Figueiredo and Pavia [33], who observed pronounced conductivity reductions at early reaction stages. RHA produced a much quicker and more pronounced drop in conductivity, falling from 7.15 to 2.63 mS/cm within 240 min, while SCBA showed a slower decline, reaching 5.66 mS/cm over the same duration. This trend suggests that, under the same test conditions, RHA demonstrates stronger short-term pozzolanic reactivity than SCBA. This behavior aligns well with previous studies that attribute the superior pozzolanic performance of RHA to its high content of amorphous silica and higher SSA (Tables 1 and 3, Figure 5) [38, 39].

By comparison, the lower but continuous conductivity loss observed in the lime–SCBA system suggests slower reaction kinetics, likely influenced by the presence of minor crystalline phases and relatively inert components. Nevertheless, the steady decrease in conductivity over time clearly confirms the pozzolanic character of SCBA [39, 56]. XRD results indicated that RHA is predominantly amorphous (Figure 5), while SCBA consists mainly of an amorphous phase with small amounts of crystalline material (Figure 1). Since amorphous silica and alumina are more soluble and reactive than their crystalline counterparts [28], these mineralogical differences account for the faster lime consumption observed in the RHA system. The conductivity measurements are consistent with the XRD findings and confirm that both ashes are suitable supplementary cementitious materials for lime-based binders, with RHA promoting rapid early reactions and SCBA contributing to sustained pozzolanic activity over longer periods.

3.5 | Water Absorption

Mortar prisms were subjected to a water absorption test for a period of up to 48 h. The results are as represented in Figure 6.

Figure 6 shows the water absorption of pure lime, lime–RHA, and lime–SCBA mortars. The pure lime mortar absorbed the most water, which reflects its highly porous structure and limited hydraulic activity [57]. Similar findings have been reported by Janotova and Slizkova [58] and Brzyski [13]. During air curing, carbonation in lime creates fine surface pores that make it easier for water to penetrate, reducing the material's durability [59]. The inherently porous nature of pure lime mortars allows them to take up significant amounts of water, which may reduce their durability by making them more susceptible to freeze–thaw action and salt buildup, as well as lead to lower early strength and a slower rate of hardening [60].

Adding agricultural waste pozzolans significantly lowered water absorption in both lime–RHA and lime–SCBA mortars, showing improved resistance to water penetration. This improvement mainly comes from pozzolanic reactions, which consume calcium hydroxide and produce additional calcium silicate hydrate gels [20]. These gels refine the pore structure, reduce connectivity between pores, and enhance long-term durability [61, 62].

TABLE 4 | Electrical conductivity of saturated $Ca(OH)_2$ solution after addition of SCBA calcined at 600°C for 2 h (initial $Ca(OH)_2$ conductivity = 7.1 mS/cm; conductivity of deionized water + SCBA = 0.66 mS/cm).

Time (min)	Electrical conductivity (mS/cm)								
	0	**30**	**60**	**90**	**120**	**150**	**180**	**210**	**240**
Average	7.15 ± 0.005	6.28 ± 0.011	6.02 ± 0.037	5.93 ± 0.033	5.89 ± 0.028	5.84 ± 0.034	5.80 ± 0.049	5.73 ± 0.040	5.66 ± 0.050

Similar reductions in water absorption and durability improvements resulting from the addition of agricultural waste additives have been widely observed in lime–pozzolana systems with RHA and SCBA [49, 63, 64].

Among the composite mortars, lime–RHA showed the lowest water absorption, which aligns with its higher pozzolanic reactivity. The high content of amorphous silica in RHA promotes extensive lime consumption and the formation of dense C–S–H networks, effectively refining the pores and limiting water movement through the mortar. This pore refinement explains the superior durability of lime–RHA mortars [65]. The lime–SCBA mortar absorbed slightly more water than lime–RHA. This is likely due to the porous and irregular shape of SCBA particles, which increase capillary porosity and water retention, especially at early ages [66]. Minor crystalline and inert phases in SCBA also slow down pozzolanic reactions, leading to less effective early-stage pore refinement compared with RHA [50]. These water absorption trends are consistent with the mineralogical and reactivity analyses in this study and demonstrate that both ashes effectively improve the durability of lime-based mortars.

3.6 | Compressive Strength Performance

The compressive and flexural strength results for the mortar mixes used in this study are summarized in Table 6 and Figures 7 and8.

The pure lime mortar had a very low 28-day compressive strength of just 0.43 MPa, reflecting the slow strength development typical of air–lime binders. These binders rely on carbonation, a gradual reaction controlled by CO_2 diffusion and moisture, which limits early and mid-term strength gain [67]. Low early-age strengths for pure lime mortars have been widely reported [67, 68]. Apostolopoulou et al. [69] reported 0.2–4.5 MPa for hydrated lime mortars. The results of the present study are within the ranges reported in this study. Nevertheless, the compressive strength measured for the pure lime mortar in this study was considerably lower than the values reported by Kaya et al. [8].

Figure 7 shows a clear increase in compressive strength when lime is mixed with agricultural waste ashes compared to pure lime mortar. The L–RHA mortar achieved a compressive strength of 4.64 MPa, which was notably higher than the value measured for the L–SCBA mortar (3.84 MPa). An independent t-test verified that this difference is statistically significant ($t(4) = 32.07$, $p < 0.0001$). Adding pozzolanic materials greatly improved the strength of pure lime mortar. The lime–RHA mortar attained 4.64 MPa, a more than tenfold increase, while L–SCBA achieved 3.84 MPa. This boost is a result of pozzolanic reactions between the amorphous silica in RHA and SCBA and the calcium hydroxide from lime hydration. This reaction produces extra C–S–H gels that densify the microstructure and reduce porosity [13, 58, 62]. The resulting denser structure not only strengthens the mortar but also enhances durability by lowering water absorption, as seen in Figure 6, where RHA mortars had the least water uptake, followed by SCBA mortars.

The superior performance of L–RHA is linked to its higher content of reactive amorphous silica and finer particle size (Table 3, Figure 5), which enable faster and more efficient pozzolanic reactions [53]. SCBA mortars, though slightly weaker, still show significant improvement over pure lime, as their

TABLE 5 | Electrical conductivity of saturated $Ca(OH)_2$ solution after addition of RHA calcined at 600°C for 2 h (initial $Ca(OH)_2$ conductivity = 7.15 mS/cm; conductivity of deionized water + RHA = 0.37 mS/cm).

Time (min)	Electrical conductivity (mS/cm)								
	0	30	60	90	120	150	180	210	240
Average	7.15 ± 0.005	4.49 ± 0.085	4.03 ± 0.108	3.69 ± 0.113	3.37 ± 0.139	3.07 ± 0.141	2.85 ± 0.103	2.73 + 0.106	2.63 ± 0.110

pozzolanic reactions continue at a slower pace due to coarser particles, minor crystalline phases, and higher residual carbon (Table 3, Figure 1) [29]. The reduced water absorption in both ashes indicates that the denser C–S–H network effectively blocks capillary water pathways, improving long-term durability. The combined gains in compressive strength and lower water absorption show that incorporating RHA and SCBA overcomes the natural limitations of pure lime. RHA provides rapid strength development and low permeability, while SCBA supports sustained long-term improvements, making both suitable for non-structural applications such as masonry mortars and rendering [56].

3.7 | Flexural Strength Performance

The flexural strength test for control and pozzolana–lime prisms is shown in Figure 8.

Figure 8 illustrates the flexural strength development of pure lime mortar in comparison with L–RHA and L–SCBA composite mortars. Pure lime mortar showed very low flexural strength (0.17 MPa), indicating its limited capacity to resist tensile and bending stresses. This response is typical of nonhydraulic lime binders, which gain strength slowly through carbonation, maintain a highly porous structure, and offer minimal resistance to crack formation and propagation [67, 68].

Flexural strength results also indicated a clear gap between the L–RHA mortar (2.70 MPa) and the lime–SCBA mortar (0.97 MPa). Statistical testing confirmed that this difference is highly significant ($t(4) = 129.5$, $p < 0.0001$). The inclusion of pozzolanic materials led to a substantial improvement in flexural strength. L–RHA achieved the highest value of 2.7 MPa, representing an increase of more than one order of magnitude compared with pure lime. This enhancement is mainly attributed to the high proportion of reactive amorphous silica in RHA, which reacts with calcium hydroxide to form secondary C–S–H phases. These products improve interparticle bonding, refine the pore structure, and increase resistance to crack initiation and growth under bending loads [13]. The strong flexural performance of L–RHA indicates the formation of a more cohesive and crack-resistant matrix, making it particularly suitable for masonry mortars, plasters, and renders, where flexural behavior strongly influences serviceability and durability.

The lime–SCBA mortar developed a flexural strength of 0.97 MPa, which, although lower than that of lime–RHA, still represents a marked improvement over pure lime. The comparatively lower performance can be linked to reduced pozzolanic reactivity arising from partially crystalline silica (Figure 2), relatively higher residual carbon content (Table 3), and possible competition between carbonation and pozzolanic reactions under air-curing conditions. In such environments, carbonation may consume calcium hydroxide that would otherwise participate in pozzolanic reactions, thereby limiting early strength development [70]. Nevertheless, SCBA still contributes to microstructural densification and progressive durability gains at later curing ages.

When compressive and flexural strengths are considered together, lime–SCBA mortars show lower ductility than pure lime, as indicated by a higher compressive-to-flexural strength ratio. Lime–RHA exhibits the highest ratio, suggesting the densest and

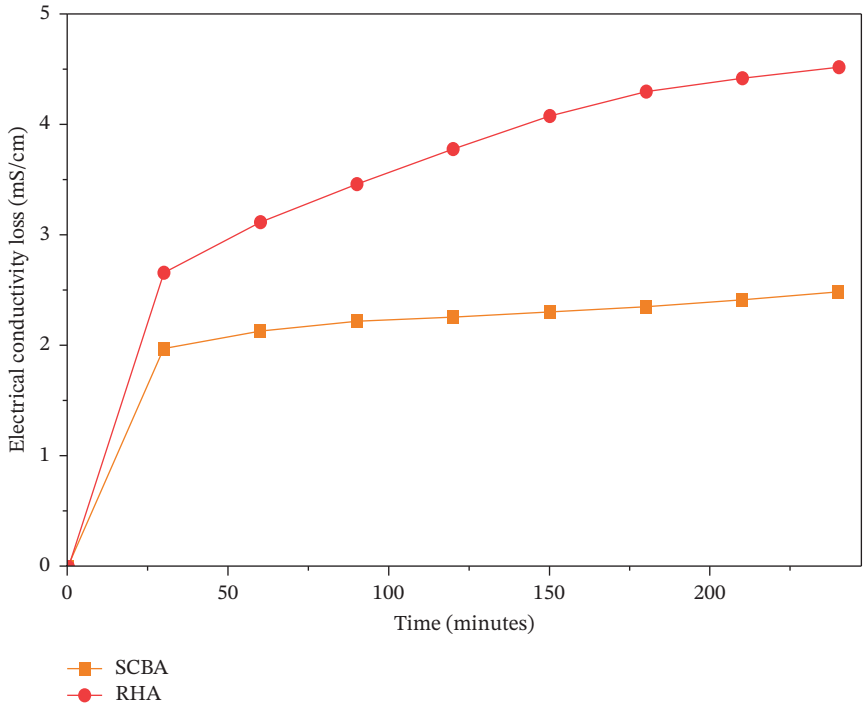

FIGURE 4 | Pozzolanic activity of RHA and SCBA samples calcined for 2 h at 600°C.

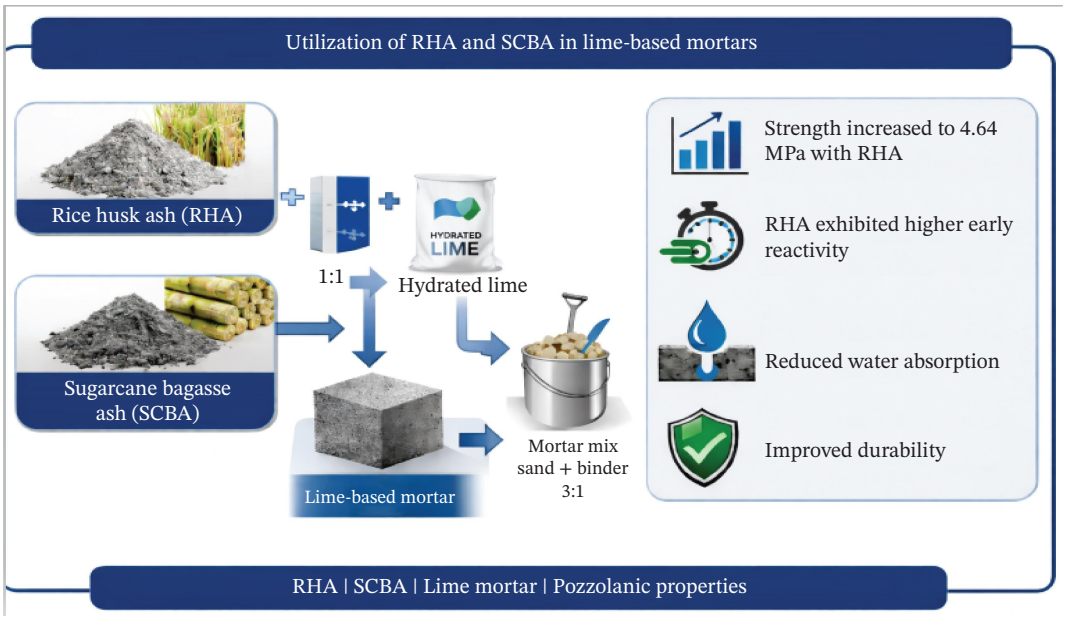

FIGURE 5 | Graphical abstract.

least ductile microstructure. This behavior is particularly important for historic masonry applications, such as rendering, plastering, and repointing, where mortars must accommodate minor movements caused by thermal changes, moisture variations, or settlement without cracking in order to ensure long-term durability [71].

The mortar specimens used for durability and mechanical testing were cured in air at approximately 60% RH to simulate realistic service conditions for lime-based mortars, where carbonation is the primary hardening mechanism. However, such conditions are not ideal for pozzolanic reactions, which require sufficient moisture to enable the dissolution of reactive silica and alumina and the transport of ions within the pore solution [71]. Reduced moisture availability limits these processes, thereby slowing the formation of strength-enhancing phases such as calcium silicate hydrate (C–S–H) and calcium aluminate hydrate (C–A–H). This effect is particularly pronounced for SCBA, which inherently exhibits slower reaction kinetics.

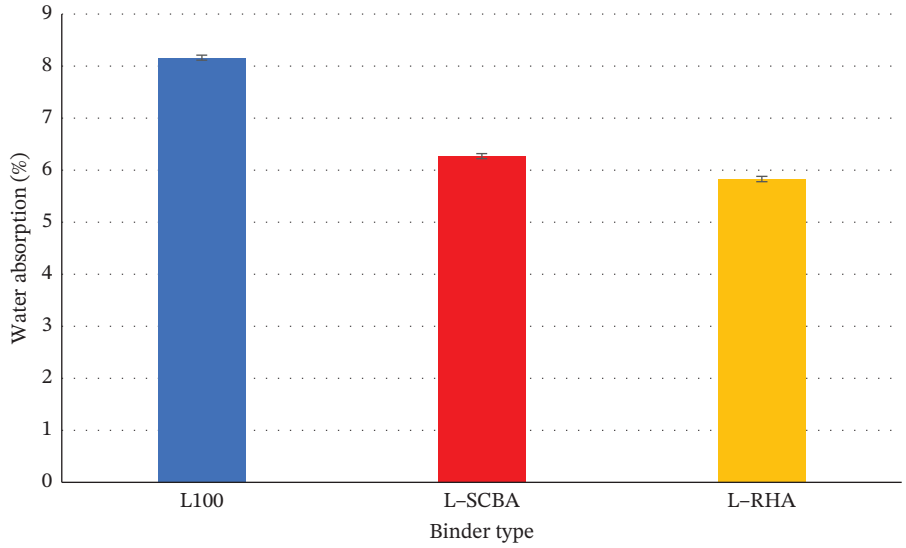

FIGURE 6 | Water absorption (%) of pure lime (L100) and pozzolan-modified (L–RHA and L–SCBA) mortars after 28 days of air curing. Error bars represent the standard deviation of triplicate measurements ($n = 3$).

TABLE 6 | Mechanical performance (compressive and flexural strength) of lime and pozzolanic-blended mortars at 28 days.

Mortar samples	Binder ratio Lime:pozz:sand	Test age (days)	Compressive strength (MPa)	Flexural strength (MPa)
Control (L100)	1:0:3	28	0.43 ± 0.06	0.17 ± 0.01
L–RHA (50/50)	1:1:3	28	$4.64 \pm 0.03^{*}$	$2.70 \pm 0.01^{*}$
L–SCBA (50/50)	1:1:3	28	$3.84 \pm 0.03^{*}$	$0.97 \pm 0.01^{*}$

Note: Values represent the mean of three specimens ($n = 3$) and the standard deviation. Asterisks (*) indicate statistical significance compared to the control ($p < 0.05$) based on a two-tailed t-test.

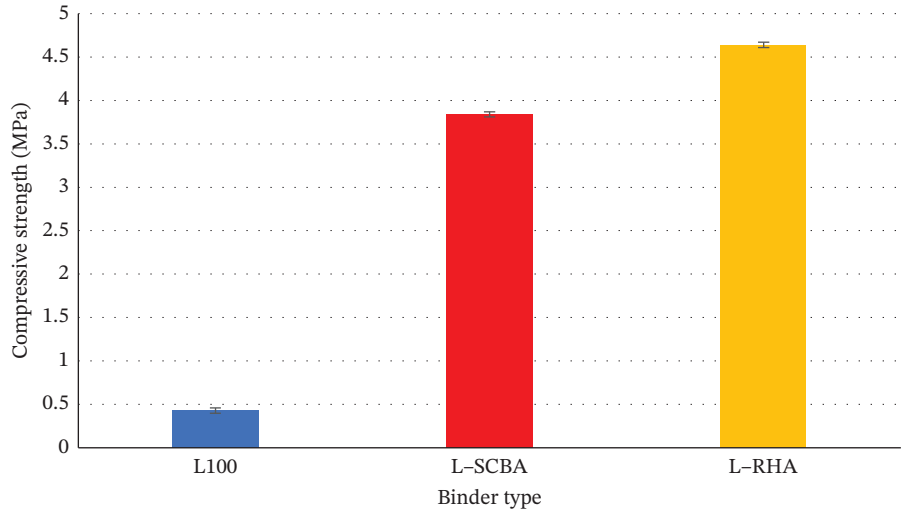

FIGURE 7 | Compressive strength (MPa) of control (L100) and pozzolan-modified (L–RHA and L–SCBA) lime mortars after 28 days of air curing. Error bars represent the standard deviation of three replicates ($n = 3$).

In addition, carbonation and pozzolanic reactions may compete under air-curing conditions, as carbonation consumes calcium hydroxide that would otherwise participate in pozzolanic reactions [70]. Consequently, the mechanical and durability properties reported in this study are likely conservative compared to those achievable under moist or high-humidity curing. Nevertheless, the selected curing regime provides a realistic assessment of in-service performance. Future work should include comparative studies under different curing conditions to better quantify the combined effects of carbonation and

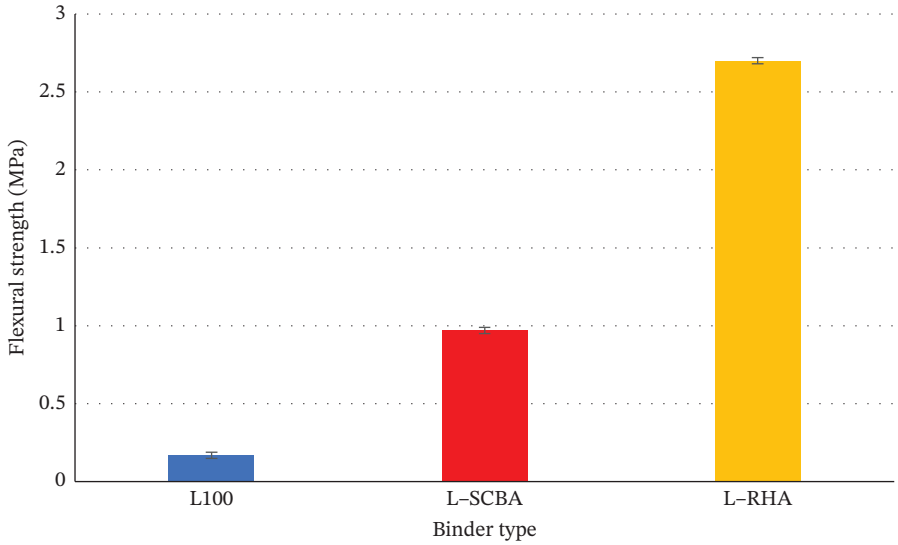

FIGURE 8 | Flexural strength (MPa) of control (L100) and pozzolan-modified (L–RHA and L–SCBA) lime mortars after 28 days of air curing. Error bars represent the standard deviation of triplicate measurements ($n = 3$).

pozzolanic activity and to identify optimal curing strategies for lime–pozzolan systems.

4 | Conclusion

Based on the results of this study, the main conclusions can be summarized as follows:

- Both RHA and SCBA exhibit strong pozzolanic characteristics, as confirmed by their chemical composition and reactivity.
- RHA demonstrates higher reactivity due to its greater amorphous silica content and finer particle size, while SCBA shows slower but sustained pozzolanic activity.
- The incorporation of both ashes significantly enhances compressive and flexural strength compared to pure lime mortars.
- RHA achieves superior mechanical performance and lower permeability, whereas SCBA provides moderate strength improvement with relatively improved flexibility.
- Water absorption is substantially reduced in modified mortars, indicating improved pore structure and durability.
- The overall performance of lime–pozzolan systems is governed by the interplay between material composition, microstructure, and reactivity.
- Lime–RHA mortars are more suitable for applications requiring higher strength and reduced permeability, such as masonry mortars and renders.
- Lime–SCBA mortars are better suited for heritage conservation and restoration works, where compatibility and flexibility are essential.
- Further studies should investigate long-term durability under aggressive environments (e.g., sulfate attack, acidic environments, and carbonation).
- Future research should also include comprehensive life cycle and cost analyses to fully quantify environmental and economic benefits.
- Environmental and economic impacts should be quantified through life cycle and cost analyses.

Author Contributions

All authors contributed significantly to this work. Odiwuor Vincent Onyango conceptualized and designed the study, conducted the experiments, analyzed data, interpreted the results, and drafted and revised the manuscript. Ayabei Kiplagat, Maurice O. Okoth, and Onesmus Mulwa Munyao provided guidance on methodology, supervised the research, and critically reviewed the manuscript.

Acknowledgments

The authors sincerely thank the University of Eldoret, the Ministry of Mining, and the Ministry of Roads for providing access to the laboratory facilities used in this work.

Funding

This research did not receive any external funding.

Disclosure

All authors read and approved the final version of the manuscript.

Conflicts of Interest

The authors declare no conflicts of interest.

Data Availability Statement

The data that support the findings of this study are available from the corresponding author upon reasonable request.

References

1. S. Krishnapriya and D. L. Venkatesh Babu, "Isolation and Identification of Bacteria to Improve the Strength of Concrete," *Microbiological Research* 174 (2015): 48–55, https://doi.org/10.1016/j.micres.2015.03.009.

2. H. F. W. Taylor, *Cement Chemistry*, 2nd ed. (Thomas Telford Publishing, 1997).

3. C. Meyer, "Concrete as a Green Building Material," in *Proceedings of the Construction Materials Mindess Symposium* (2005).

4. A. Tahsin, W. Ashraf, and I. B. Borno, "Influence of Different Lime Sources on the Properties and Environmental Impacts of Seawater-Activated Lime-Calcined Clay Binder," *Journal of Sustainable Cement-Based Materials* 14, no. 5 (2025): 1–12, https://doi.org/10.1080/21650373.2025.2476772.

5. J. M. Abed, M. Al-Gburi, and A. Almssad, "Evaluation of Physical and Mechanical Properties of Modified Cement-Lime Mortar Containing Recycled Granite Powder Waste as a Partial Fine Aggregate Replacement," *Applied Sciences* 14, no. 22 (2024): 10146, https://doi.org/10.3390/app142210146.

6. S. Pavia, "An Assessment of Lime Mortars for Masonry Repair," *Academia.edu* (2006).

7. P. Brzyski, Z. Suchorab, and G. Łagód, "The Influence of Casein Protein Admixture on Pore Size Distribution and Mechanical Properties of Lime-Metakaolin Paste," *Buildings* 11, no. 11 (2021): 530, https://doi.org/10.3390/buildings11110530.

8. Y. Kaya, N. Mardani, A. Mardani, A. Doğangün, and A. Doğangün, "Improving Lime-Based Restoration Mortars: Effect of Type and Utilization Rate of Binder and Aggregate," *Materials* 18, no. 5 (2025): 961, https://doi.org/10.3390/ma18050961.

9. N. Chousidis and G. Batis, "Reducing CO_2 Emissions in Urban Infrastructure: The Role of Siliceous Fly Ash in Sustainable Mortar Design," *Sustainability* 17, no. 11 (2025): 4835, https://doi.org/10.3390/su17114835.

10. N. Singh, "Fly Ash-Based Geopolymer Binder: A Future Construction Material," *Minerals* 8, no. 7 (2018): 299, https://doi.org/10.3390/min8070299.

11. M. R. Mondhe, R. Prasad, and S. G. Makarande, "Utilization of Industrial Wastes in Mortar (Silica Fume & Flyash)," *International Journal of Engineering Research and Technology* 2, no. 7 (2013).

12. A. Kumar, N. Bheel, I. Ahmed, S. H. Rizvi, R. Kumar, and A. A. Jhatial, "Effect of Silica Fume and Fly Ash as Cementitious Material on Hardened Properties and Embodied Carbon of Roller Compacted Concrete," *Environmental Science and Pollution Research* 28 (2021).

13. P. Brzyski, "The Effect of Pozzolan Addition on the Physical and Mechanical Properties of Lime Mortar," *E3S Web of Conferences* 49 (2018): 00009, https://doi.org/10.1051/e3sconf/20184900009.

14. A. Shukla, K. Kishore, and N. Gupta, "Mechanical Properties of Cement Mortar With Lime & Rice Husk Ash," *IOP Conference Series: Materials Science and Engineering* 1116, no. 1 (2021): 012025.

15. S. Nassiri, A. A. Butt, A. Zarei, et al., "Opportunities for Supplementary Cementitious Materials From Natural Sources and Industrial Byproducts: Literature Insights and Supply Assessment," *Buildings* 15, no. 17 (2025): 3099, https://doi.org/10.3390/buildings15173099.

16. Ms. Duhita and H. Doye, "Green Concrete: Efficient & Eco-Friendly Construction Materials," *IOSR Journal of Mechanical and Civil Engineering* 14, no. 03 (2017): 33–35.

17. M. A. Khan, B. Zhang, M. Ahmad, et al., "Optimizing Concrete Sustainability With Bagasse Ash and Stone Dust and Its Impact on Mechanical Properties and Durability," *Scientific Reports* 15, no. 1 (2025): 1385, https://doi.org/10.1038/s41598-025-85363-x.

18. N. Elawadly and S. A. Sanad, "Sustainable Concrete Incorporating Sugarcane Bagasse Ash: A Study on Workability, Mechanical Behavior, and Microstructure," *Innovative Infrastructure Solutions* 10, no. 9 (2025): 401, https://doi.org/10.1007/s41062-025-02177-6.

19. KS EAS 18-1, *Kenya Standard Test Method for Oxides Specification of Hydraulic Cement* (KEBS, 2017).

20. M. P. Luxán, F. Madruga, and J. Saavedra, "Rapid Evaluation of Pozzolanic Activity of Natural Products by Conductivity Measurement," *Cement and Concrete Research* 19, no. 1 (1989): 63–68, https://doi.org/10.1016/0008-8846(89)90066-5.

21. KS EAS 2168-1, *Kenya Standard Test Method, Composition, Specification, and Conformity Criteria of Masonry Cement* (KEBS, 2020).

22. ASTMC109/C109M-21, *Standard Test Method for Compressive Strength of Hydraulic Cement Mortars* (ASTM International, 2020).

23. L. Schnabel, "Lectures on Materials Science for Architectural Conservation," *Studies in Conservation* 59, no. 2 (2014): 123–124, https://doi.org/10.1179/0039363014z.000000000151.

24. J. Monteiro, V. Silva, and P. Faria, "Effect of Type of Curing and Metakaolin Replacement on Air Lime Mortars for the Durability of Masonries," *Infrastructure* 6, no. 10 (2021): 143, https://doi.org/10.3390/infrastructures6100143.

25. BS 1881-122, *Method for Determination of Water Absorption* (British Standard Institution, 2011).

26. Kenya Bureau of Standards, *Cement Test Methods Part 1: Determination of Strength* (KS EAS, 2000).

27. EN196-1, *Methods of Testing Cement—Part 1: Determination of Strength* (iTeh, Inc, 2016).

28. R. Walker and S. Pavía, "Physical Properties and Reactivity of Pozzolans, and Their Influence on the Properties of Lime–Pozzolan Pastes," *Materials and Structures* 44, no. 6 (2010): 1139–1150, https://doi.org/10.1617/s11527-010-9689-2.

29. G. C. Cordeiro, R. D. Toledo Filho, and E. de Moraes Rego Fairbairn, "Use of Ultrafine Rice Husk Ash With High-Carbon Content as Pozzolan in High-Performance Concrete," *Materials and Structures* 42, no. 7 (2008): 983–992, https://doi.org/10.1617/s11527-008-9437-z.

30. J. M. Marangu, "Physico-Chemical Properties of Kenyan-Made Calcined Clay-Limestone Cement (LC3)," *Case Studies in Construction Materials* 12 (2020): e00333, https://doi.org/10.1016/j.cscm.2020.e00333.

31. G. A. Habeeb and H. B. Mahmud, "Study on Properties of Rice Husk Ash and Its Use as Cement Replacement Material," *Materials Research* 13, no. 2 (2010): 185–190, https://doi.org/10.1590/s1516-14392010000200011.

32. N. Yaseen, "Exploring the Potential of Sugarcane Bagasse Ash as a Sustainable Supplementary Cementitious Material: Experimental Investigation and Statistical Analysis," *Results in Chemistry* 10 (2024): 101723, https://doi.org/10.1016/j.rechem.2024.101723.

33. R. L. Figueiredo and S. Pavia, "A Study of the Parameters That Determine the Reactivity of Sugarcane Bagasse Ashes (SCBA) for Use as a Binder in Construction," *SN Applied Sciences* 2, no. 9 (2020): 1515, https://doi.org/10.1007/s42452-020-03224-w.

34. G. A. Habeeb and M. Fayyadh, "Rice Husk Ash Concrete: The Effect of RHA Average Particle Size on Mechanical Properties and Drying Shrinkage," *Australian Journal of Basic and Applied Sciences* 3, no. 3 (2009): 1616–1622.

35. B. I. Rasoul, F. K. Günzel, and M. I. Rafiq, *Effect of Rice Husk Ash Properties on the Early Age and Long-Term Strength of Mortar* (2018).

36. ASTM C618, "Standard Specification for Coal Fly Ash and Raw or Calcined Natural Pozzolan for Use in Concrete" (1999).

37. P. K. Mehta, *Rice Husk Ash—A Unique Supplementary Cementing Material. CANMET, Ottawa, Canada, MSL Report 94-1 (R)* (References—Scientific Research Publishing, 1994).

38. L. K. John, "Pozzolana Cement Obtained by Calcining Raw Clays/Rice Husks Mixtures" (2013).

39. O. Assumptor, E. Masika, K. Thiong, and N. Kenya, "Probing Optimal Blends of Pozzolans to Develop Supplementary Cementing Material Within Busia County, Kenya," *Journal of Applied Physics* 12, no. 2 (2020): 59–69.

40. M. S. Rodrigues, J. Payá, L. Soriano, H. Savastano, and A. L. Beraldo, "Study of the Pozzolanic Reactivity of Sugar Cane Straw Ashes (SCSA) Burned Under Controlled Conditions," *Materials* 16, no. 21 (2023): 6841, https://doi.org/10.3390/ma16216841.

41. B. A. Silva, E. Guerreiro, and A. P. C. Duarte, "Comparative Study of Lime-Based Mortars for Conservation and Restoration Interventions," *Construction and Building Materials* 499 (2025): 143956, https://doi.org/10.1016/j.conbuildmat.2025.143956.

42. T. Al-Attar and Z. Al-Azzawi, "Evaluation of Pozzolime Mixtures as a Sustainable Binder to Replace Portland Cement in Structural Concrete," *MATEC Web of Conferences* 120 (2017): 02009.

43. N. Hammad, I. G. Shaaban, and A. El-Nemr, "The Efficiency of Calcium Oxide on Microbial Self-Healing Activity in Alkali-Activated Slag (AAS)," *Applied Sciences* 14, no. 12 (2024): 5299, https://doi.org/10.3390/app14125299.

44. A. M. Neville, *Properties of Concrete* (Pearson Education Limited, 2011).

45. A. Kamalakar Mali and P. Nanthagopalan, "Development of a Framework for the Selection of Best Sugarcane Bagasse Ash From Different Sources for Use in the Cement-Based System: A Rapid and Reliable Path," *Construction and Building Materials* 293 (2021): 123386, https://doi.org/10.1016/j.conbuildmat.2021.123386.

46. EN 459-1, *Building Lime. Definitions, Specifications, and Conformity Criteria* (European Committee for Standardization (CEN), 2010).

47. R. G. Newton and J. H. Sharp, "The Chemical Composition of Lime Plasters," *Cement and Concrete Research* 17, no. 1 (1987): 77–80, https://doi.org/10.1016/0008-8846(87)90061-5.

48. A. Padovnik and V. Bokan-Bosiljkov, "The Influence of Dry Hydrated Limes on the Fresh and Hardened Properties of Architectural Injection Grout," *Materials* 14, no. 19 (2021): 5585, https://doi.org/10.3390/ma14195585.

49. K. Ganesan, K. Rajagopal, and K. Thangavel, "Rice Husk Ash Blended Cement: Assessment of Optimal Level of Replacement for Strength and Permeability Properties of Concrete," *Construction and Building Materials* 22, no. 8 (2008): 1675–1683, https://doi.org/10.1016/j.conbuildmat.2007.06.011.

50. M. Frías, E. Villar-Cociña, and E. Valencia-Morales, "Characterization of Sugarcane Straw Waste as Pozzolanic Material for Construction: Calcining Temperature and Kinetic Parameters," *Waste Management* 27, no. 4 (2007): 533–538, https://doi.org/10.1016/j.wasman.2006.02.017.

51. BS EN 197-1, *Cement Part 1: Composition, Specifications, and Conformity Criteria for Common Cements* (British Standard Institute, London, 2011).

52. S. Kumar Das, A. Adediran, C. Rodrigue Kaze, S. Mohammed Mustakim, and N. Leklou, "Production, Characteristics, and Utilization of Rice Husk Ash in Alkali Activated Materials: An Overview of Fresh and Hardened State Properties," *Construction and Building Materials* 345, no. 128341 (2022): https://doi.org/10.1016/j.conbuildmat.2022.128341.

53. M. H. Zhang, R. Lastra, and V. M. Malhotra, "Rice-Husk Ash Paste and Concrete: Some Aspects of Hydration and the Microstructure of the Interfacial Zone Between the Aggregate and Paste," *Cement and Concrete Research* 26, no. 6 (1996): 963–977, https://doi.org/10.1016/0008-8846(96)00061-0.

54. A. Arizzi and G. Cultrone, "The Influence of Aggregate Texture, Morphology, and Grading on the Carbonation of Non-Hydraulic (Aerial) Lime-Based Mortars," *Quarterly Journal of Engineering Geology and Hydrogeology* 46, no. 4 (2013): 507–520, https://doi.org/10.1144/qjegh2012-017.

55. T. Matschei, B. Lothenbach, and F. P. Glasser, "The Role of Calcium Carbonate in Cement Hydration," *Cement and Concrete Research* 37, no. 4 (2007): 551–558, https://doi.org/10.1016/j.cemconres.2006.10.013.

56. E. Villar-Cociña, E. Valencia-Morales, R. González-Rodríguez, and J. Hernández-Ruíz, "Kinetics of the Pozzolanic Reaction Between Lime and Sugar Cane Straw Ash by Electrical Conductivity Measurement: A Kinetic–Diffusive Model," *Cement and Concrete Research* 33, no. 4 (2003): 517–524, https://doi.org/10.1016/s0008-8846(02)00998-5.

57. J. Bartholdy, M. R. Midtgaard, I. Rörig-Dalgaard, and M. Taube, "Water Absorption in Medieval Lime Plaster: Influence of Binder Ratio, Preparation Protocol, and Limewashing," *Construction and Building Materials* 486 (2025): 141946, https://doi.org/10.1016/j.conbuildmat.2025.141946.

58. D. Janotova and Z. Slizkova, "Lime-Based Mortars With Various Binder Compositions: Characterization and Freeze-Thaw Resistance Assessment," *IOP Conference Series: Materials Science and Engineering* 1205 (2021): 1012009.

59. R. Malathy, R. Shanmugam, S. H. Kim, I.-M. Chung, and M. Prabakaran, "Mechanical and Microstructural Properties of Composite Mortars With Lime, Silica Fume, and Rice Husk Ash," *Processes* 10, no. 7 (2022): 1424, https://doi.org/10.3390/pr10071424.

60. T. B. Su-Cadirci, J. Calabria-Holley, C. Ince, and R. J. Ball, "Freeze-Thaw Resistance of Pozzolanic Hydrated Lime Mortars," *Construction and Building Materials* 394 (2023): 131993, https://doi.org/10.1016/j.conbuildmat.2023.131993.

61. A. A. de Siqueira and G. C. Cordeiro, "Sustainable Cements Containing Sugarcane Bagasse Ash and Limestone: Effects on Compressive Strength and Acid Attack of Mortar," *Sustainability* 14, no. 9 (2022): 5683, https://doi.org/10.3390/su14095683.

62. A. Hamza, S. Derogar, and C. Ince, "The Effects of Silica Fume and Hydrated Lime on the Strength Development and Durability Characteristics of Concrete Under Hot Water Curing Conditions," *MATEC Web of Conferences* 120 (2017): 02004, https://doi.org/10.1051/matecconf/201712002004.

63. G. R. Sensale, "Effect of Rice-Husk Ash on Durability of Cementitious Materials," *Cement and Concrete Composites* 32, no. 9 (2010): 718–725, https://doi.org/10.1016/j.cemconcomp.2010.07.008.

64. J. da S. Andrade Neto, M. J. S. de França, N. S. de Amorim Júnior, and D. V. Ribeiro, "Effects of Adding Sugarcane Bagasse Ash on the Properties and Durability of Concrete," *Construction and Building Materials* 266 (2021): 120959, https://doi.org/10.1016/j.conbuildmat.2020.120959.

65. P. A. Adesina and F. A. Olutoge, "Structural Properties of Sustainable Concrete Developed Using Rice Husk Ash and Hydrated Lime," *Journal of Building Engineering* 25 (2019): 100804, https://doi.org/10.1016/j.jobe.2019.100804.

66. L. Mirzaei, T. Ghebrab, and C. B. Fedler, "Review and Evaluation of Agricultural Biomass Ashes as Supplementary Cementitious Materials for Sustainable Concrete," *Processes* 13, no. 11 (2025): 3571, https://doi.org/10.3390/pr13113571.

67. R. Michael and H. Lawrence, "A Study of Carbonation in Non-Hydraulic Lime Mortars" (2006).

68. K. Elert, C. Rodriguez-Navarro, E. S. Pardo, E. Hansen, and O. Cazalla, "Lime Mortars for the Conservation of Historic Buildings," *Studies in Conservation* 47, no. 1 (2002): 62–75, https://doi.org/10.1179/sic.2002.47.1.62.

69. M. Apostolopoulou, A. Bakolas, and M. Kotsainas, "Mechanical and Physical Performance of Natural Hydraulic Lime Mortars," *Construction and Building Materials* 290 (2021): 123272, https://doi.org/10.1016/j.conbuildmat.2021.123272.

70. Ö. Cizer, K. Van Balen, and D. Van Gemert, "Competition Between Hydration and Carbonation in Hydraulic Lime and Lime-Pozzolana Mortars," *Advanced Materials Research* 133–134 (2010): 241–246, https://doi.org/10.4028/www.scientific.net/amr.133-134.241.

71. B. A. Silva, A. P. Ferreira Pinto, and A. Gomes, "Natural Hydraulic Lime Versus Cement for Blended Lime Mortars for Restoration Works," *Construction and Building Materials* 94 (2015): 346–360, https://doi.org/10.1016/j.conbuildmat.2015.06.058.